Spectra of non-Hermitian quantum spin chains describing boundary induced phase transitions

1997 J. Phys. A: Math. Gen. 30 4925

(http://iopscience.iop.org/0305-4470/30/14/008)

J. Phys. A: Math. Gen. **30** (1997) 4925–4938. Printed in the UK PII: S0305-4470(97)80130-8

Spectra of non-Hermitian quantum spin chains describing boundary induced phase transitions

Ulrich Bilstein† and Birgit Wehefritz‡

Universität Bonn, Physikalisches Institut, Nußallee 12, D-53115 Bonn, Germany

Received 5 December 1996, in final form 1 April 1997

Abstract. The spectrum of the non-Hermitian asymmetric XXZ-chain with additional non-diagonal boundary terms is studied. The lowest-lying eigenvalues are determined numerically. For the ferromagnetic chain the temporal correlation length shows the same properties as the spatial correlation length. For the antiferromagnetic chain, we find a conformal invariant spectrum where the partition function corresponds to the one of a Coulomb gas with only magnetic charges. This is in contrast to the case of diagonal boundary terms where one finds only electric charges. Similar results are obtained in a toy model that can be diagonalized analytically in terms of free fermions.

1. Introduction

In the study of reaction-diffusion processes non-Hermitian chains appear in a natural way. However, their properties have not yet been studied extensively. For instance, the effect of boundary conditions on the spectrum of non-Hermitian Hamiltonians is unknown. In this article we study an asymmetric XXZ-chain with modified boundary terms and we show that these boundary terms give rise to new and interesting features.

In this article two examples are treated that both show the appearance of boundary-induced phase transitions. As a first example, we study the Hamiltonian of the asymmetric diffusion model on a one-dimensional lattice with open boundaries, injection and ejection of particles at the edges of the chain. In this model, particles of one species can diffuse on the lattice with length N with a rate p to the right and q to the left. Particles are injected at the left boundary with a rate α and extracted with a rate β at the right boundary. The Hamiltonian of this model is given by the following expression [1]:

$$H = -\sum_{j=1}^{N-1}\left[q\sigma_j^-\sigma_{j+1}^+ + p\sigma_j^+\sigma_{j+1}^- + \frac{p+q}{4}(\sigma_j^z\sigma_{j+1}^z - 1) + \frac{q-p}{4}(\sigma_{j+1}^z - \sigma_j^z)\right] + B_1 + B_N \tag{1.1}$$

with

$$B_1 = \frac{\alpha}{2}(\sigma_1^z - 2\sigma_1^- + 1) \qquad \text{and} \qquad B_N = -\frac{\beta}{2}(\sigma_N^z + 2\sigma_N^+ - 1). \tag{1.2}$$

† E-mail address: bilstein@theoa1.physik.uni-bonn.de
‡ E-mail address: birgit@theoa1.physik.uni-bonn.de

0305-4470/97/144925+14$19.50

The bulk term of this Hamiltonian corresponds to the asymmetric XXZ-Hamiltonian. This model, and versions of it, have been studied extensively [1–7], but very few results are known about its temporal evolution.

The first part of this article deals with the analysis of the spectrum of H for $q = 0$. The Hamiltonian is known to be integrable [8], but because of the lack of a reference state, the Bethe ansatz equations have not yet been obtained. Therefore numerical methods are applied here. We were interested in determining the correspondence between the spatial correlation lengths already known from previous work [2, 3] and the dynamical properties of the Hamiltonian, i.e. the time correlation length τ given by the inverse of the smallest energy gap E_G. E_G is determined for lattice lengths of $2 \leqslant N \leqslant 18$ sites and then extrapolated to the thermodynamical limit. The boundary induced phase diagram known for the stationary state [3, 2] is reproduced by the spectrum of the Hamiltonian which is not always the case [9].

The second part of the paper is devoted to the antiferromagnetic version of the Hamiltonian. It can be obtained from the logarithmic derivative of the transfer matrix of the six-vertex model [10] and it can be used to describe the equilibrium shape of a crystal [11]. The phase diagram of the antiferromagnetic chain with periodic boundary conditions has recently been determined [12], partition functions for this system were derived in [13]. The boundary conditions we analyse in this paper (with additional non-diagonal boundary terms) have not been treated before. Our new results are obtained by determining the lowest-lying eigenvalues of the Hamiltonian up to 18 sites in the general case and 21 sites in the CP-invariant case ($\alpha = \beta$) using a version of the deflated Arnoldi algorithm [14]. The Arnoldi algorithm was already used for the study of non-Hermitian quantum chains in [15] whereas a Lanczos technique was used in [16].

The analysis of the spectrum for $p > q$ and $\alpha, \beta > 0$ suggests surprisingly the partition function of a Coulomb gas [17] that has only magnetic charges m

$$\mathcal{Z} = \lim_{N\to\infty} \operatorname{tr} z^{\frac{N}{\pi\xi}(H - f_\infty - e_\infty N)} = z^{-\frac{1}{24}} \sum_{m\in\frac{\mathbb{Z}}{2}} z^{R^2(m+\mathrm{i}(x+Ny))^2} \Pi_V(z) \tag{1.3}$$

with

$$\Pi_V(z) = \prod_{i=1}^{\infty} (1 - z^i)^{-1}. \tag{1.4}$$

Notice that the magnetic charge m is shifted by the amount $\mathrm{i}(x + Ny)$ where x depends on both bulk and boundary parameters whereas y is a function of the bulk ones only.

For lattices with an even (odd) number of sites m takes half-integer (integer) values. Since for $\alpha\beta = 0$ the spectrum is massive, we can conclude that the boundary terms give rise to the conformal invariant structure of the spectrum.

We also studied a toy model consisting of a simplified version of the Hamiltonian (1.1) that can be diagonalized in terms of free fermions. Analytic calculations give similar results to those previously obtained by numerical calculations.

This paper is organized as follows. In section 2, we define the model. We present our numerical results for the temporal correlation length in section 3 and compare them with the phase diagram of the stationary state and the known expressions for spatial correlation lengths. Section 4 deals with the antiferromagnetic case. The finite-size scaling behaviour of the lowest-lying energy levels suggests the partition function (1.3). In section 5 we present our analytical results obtained by diagonalization of the toy model which reproduces the results of section 4. Section 6 closes the paper with a discussion on our results.

2. Asymmetric diffusion model with boundary terms

We consider a model defined on a chain with N sites. Each site can be either occupied by a particle of species A or empty. For the dynamics we consider only processes that involve two neighbouring sites. The following processes are allowed:

$$\begin{aligned} &\text{diffusion to the right: } A+0 \to 0+A \qquad \text{with rate } p \\ &\text{diffusion to the left: } 0+A \to A+0 \qquad \text{with rate } q. \end{aligned} \tag{2.1}$$

Additionally we allow processes that occur only at the two edges of the chain:

$$\begin{aligned} &\text{injection at the left edge: } 0 \to A \qquad \text{with rate } \alpha \\ &\text{extraction at the right edge: } A \to 0 \qquad \text{with rate } \beta. \end{aligned} \tag{2.2}$$

The time evolution of the system is described by a master equation [18] for the probability distribution $P(\{\gamma\},t)$ to find a configuration $\{\gamma\}$ of occupied and empty sites on the lattice at time t

$$\frac{\partial}{\partial t}P(t) = -HP(t). \tag{2.3}$$

The corresponding Hamiltonian is given by (1.1). It is trivial to see that the spectrum of H is unchanged by the transformation $\alpha \leftrightarrow \beta$. In particular if $\alpha = \beta$, the Hamiltonian is invariant under the transformation particle $\leftrightarrow$ vacancy together with a reflection (CP-symmetry). Through a similarity transformation [5] the Hamiltonian (1.1) can be brought to the familiar form:

$$\begin{aligned} H' = -\frac{\sqrt{pq}}{2}\sum_{j=1}^{N-1}\Bigg[&\sigma_j^x\sigma_{j+1}^x + \sigma_j^y\sigma_{j+1}^y + \frac{\mathcal{Q}+\mathcal{Q}^{-1}}{2}(\sigma_j^z\sigma_{j+1}^z - 1) \\ &+ \frac{\mathcal{Q}-\mathcal{Q}^{-1}}{2}(\sigma_{j+1}^z - \sigma_j^z)\Bigg] + B_1' + B_N' \end{aligned} \tag{2.4}$$

with $\mathcal{Q} = \sqrt{\frac{q}{p}}$ and arbitrary Λ. This is the $U_{\mathcal{Q}}SU(2)$ invariant Hamiltonian [19] with $\Delta = \frac{\mathcal{Q}+\mathcal{Q}^{-1}}{2}$ and boundary terms:

$$B_1' = \frac{\alpha}{2}(\sigma_1^z - 2\mathcal{Q}^{\frac{1-N}{2}}\sigma_1^- + 1) \qquad B_N' = -\frac{\beta}{2}(\sigma_N^z + 2\mathcal{Q}^{\frac{1-N}{2}}\sigma_N^+ - 1).$$

Notice that their non-Hermitian part only influences the spectrum if both boundary terms are present ($\alpha\beta \neq 0$). Notice also the N-dependence of B_1' and B_N'.

3. Results for the total asymmetric diffusion model with boundary terms

3.1. Analytical results for the stationary state

For future reference, let us first present some of the results achieved previously for the total asymmetric diffusion model ($p = 1$, $q = 0$). In [2, 3] the phase diagram for the current and the spatial profile of the concentration have been determined as functions of α and β. The phase diagram is given in figure 1.

The density profile of the concentration in the stationary state obtained in [2, 3] allows us to read off the spatial correlation length ξ in the different phases [3]. One observes that in phases A_1 and B_1, ξ depends on α and β while it depends only on α in phase B_2 and only on β in phase A_2. In phase C and on the coexistence line the one-point function $\langle n_k \rangle$ shows an algebraic behaviour.

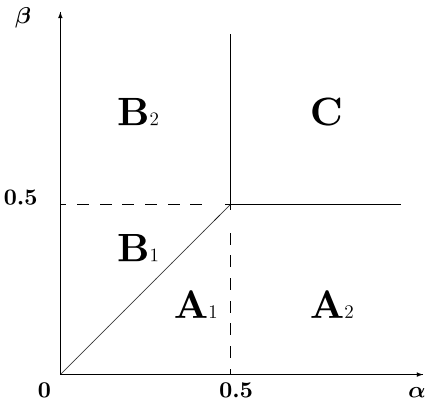

Figure 1. Phase diagram for the total asymmetric diffusion model [3].

3.2. Numerical results for the time correlation length

In this section we compare the phase structure of the stationary state with the spectrum of the Hamiltonian. We investigate the gap between the ground state and the first excited state of the spin chain. This energy gap E_G allows us to read off the time correlation length τ directly:

$$\tau^{-1} \simeq E_G. \tag{3.1}$$

We determine the lowest-lying excitation energies for lattice lengths $2 \leqslant N \leqslant 18$ by diagonalizing the Hamiltonian numerically, using a version of the deflated Arnoldi algorithm [14]. The eigenvalues were then extrapolated with the help of the BST algorithm [20]. α and β have been varied in steps of 0.1 between 0.1 and 1. The following form of the energy gap has been found in the different regions of the phase diagram. In phases A_1 and B_1, E_G is a function of α and β, while in phase B_2, E_G depends only on α and in phase A_2, depends only on β. In phase C and on the coexistence line the system is massless:

$$\begin{aligned} &A_1 : E_G = m(\alpha, \beta) \\ &A_2 : E_G = m(\beta) \\ &B_1 : E_G = m(\alpha, \beta) \\ &B_2 : E_G = m(\alpha) \\ &C : E_G \sim N^{-\frac{3}{2}} \\ &\alpha = \beta < \tfrac{1}{2} : E_G \sim N^{-2}. \end{aligned} \tag{3.2}$$

Here m denotes the mass of the spectrum.

Table 1 shows extrapolants for the energy gaps. One sees clearly that in phase B_1 the energy gap depends on both α and β while it depends only on α in phase B_2. We did not give any extrapolants for phases A_1 and A_2 since the spectrum is symmetric under permutation of α and β as described in section 2. Table 1 also shows that the mass gap vanishes in phase C and on the coexistence line. In table 2 extrapolants for the exponent $\frac{3}{2}$ in phase C and for the exponent 2 on the coexistence line can be found.

Comparing these results with the behaviour of the spatial correlation length, we can see that the temporal correlation length shows the same behaviour as the spatial correlation length in the different phases: in phase C and on the coexistence line τ diverges algebraically

Table 1. Asymmetric diffusion model: Dependence of the extrapolated gap E_G on α and β. Negative values indicate that errors are of the order of 10^{-5}.

$\beta \setminus \alpha$	0.1	0.2	0.3	0.4	0.5	0.6	0.7	0.8	0.9	1.0
1.0	0.125 73	0.040 14	0.010 17	0.001 19	0.000 00	0.000 01	−0.000 02	−0.000 01	−0.000 00	0.000 00
0.9	0.125 75	0.040 14	0.010 21	0.001 18	−0.000 03	0.000 00	−0.000 04	−0.000 01	−0.000 00	
0.8	0.125 73	0.040 13	0.010 19	0.001 18	−0.000 01	0.000 00	−0.000 04	−0.000 04		
0.7	0.125 87	0.040 12	0.010 19	0.001 14	−0.000 03	−0.000 02	−0.000 04			
0.6	0.120 17	0.040 16	0.010 30	0.001 20	−0.000 01	−0.000 01				
0.5	0.099 99	0.033 31	0.008 61	0.001 10	0.00000					
0.4	0.072 13	0.020 18	0.003 30	−0.000 05						
0.3	0.041 73	0.006 78	−0.000 01							
0.2	0.014 28	−0.000 01								
0.1	−0.000 00									

Table 2. Asymmetric diffusion model: Extrapolated exponents of the first excited state.

$\beta \setminus \alpha$	0.1	0.2	0.3	0.4	0.5	0.6	0.7	0.8	0.9	1.0
1.0					1.500 0	1.470	1.456	1.480	1.4999	1.522
0.9					1.499	1.452	1.503	1.4994	1.4999	
0.8					1.499 7	1.430	1.436	1.499		
0.7					1.462	1.405	1.499			
0.6					1.434	1.377				
0.5					1.499 99					
0.4				2.01						
0.3			1.98							
0.2		2.010								
0.1	1.992									

for $N \to \infty$ while it remains finite in phases A and B. The exponent $\frac{3}{2}$ has also been found for the total asymmetric diffusion model with periodic boundary conditions [6]. The periodic model can be mapped onto a model for surface growth [21]. This mapping can be formulated analogously for the open chain with additional boundary terms that are treated here. Then, in the language of growth models, the exponent $\frac{3}{2}$ describes KPZ-type growth [22]. The exponent 2 we find on the coexistence line can be understood by considering the diffusive motion of 'domain walls' which separate a region which has a high density of particles from a region of low density. These domain walls move like a random walker, thus leading to the above exponent [23].

In phases A_2 and B_2, τ depends only on β or α respectively. However, the numerical values for the temporal correlation length are different from those for the spatial correlation length.

Similar properties for the spatial and the temporal correlation length have been found in [24] where time-dependent correlation functions are computed for the totally asymmetric diffusion model with parallel dynamics. On the line $\alpha = \beta$ that extends in this case up to the point $\alpha = \beta = 1$ an exponent 2 is also found. The physical properties can only be compared with the model studied in this paper for $\alpha, \beta < \frac{1}{2}$.

The fact that the temporal evolution of the system reflects itself in the stationary state (for $t \to \infty$) is not yet understood. This is not true in general, as there are examples for a different behaviour of the spatial and the temporal correlation length [9].

4. The antiferromagnetic case

The low-lying excitations of the ferromagnetic chain correspond to the highest states of the antiferromagnetic chain and vice versa. The numerical studies concentrate on the case $q = 0$ and $p = 1$ with $\alpha, \beta \geqslant 0$.

The analysis of the spectrum suggests that it corresponds to a conformal invariant theory. For conformal invariant systems, the ground state takes the following form for finite lattices and open boundary conditions [25]:

$$\frac{E_0(N)}{N} = e_\infty + \frac{f_\infty}{N} - \frac{\pi \xi c}{24N^2} - \mathrm{o}(N^{-2}). \tag{4.1}$$

The energy gaps scale here as

$$\mathcal{E}_r = \lim_{N\to\infty} \frac{N}{\pi\xi}(E_r(N) - E_0(N)) = (\Delta + r). \tag{4.2}$$

Here ξ is a normalization constant and c is the central charge of the Virasoro algebra.

We have considered separately lattices with even and odd numbers of sites. Since the ground state was calculated from an odd number of sites, we used interpolated values from odd lattice lengths for the values of the ground state for even lattice lengths. While the ground-state energy is real for all lattice lengths, most of the excited states have a non-vanishing imaginary part. This is a feature that has already appeared for the periodic asymmetric XXZ-chain [13] and in the calculation of the operator content of the five-vertex model defined on an anisotropic lattice [26].

We considered the imaginary part of the energy gap

$$\mathcal{I} = \lim_{N\to\infty} \frac{1}{\pi\xi} \mathrm{Im}(E(N)) \tag{4.3}$$

the correction to the real part

$$\mathrm{Re}(\mathcal{E}) = \lim_{N\to\infty} \frac{N}{\pi\xi} \mathrm{Re}(E(N) - E_0(N))) \tag{4.4}$$

and the correction to the imaginary part

$$\mathrm{Im}(\mathcal{E}) = \lim_{N\to\infty} \frac{N}{\pi\xi} \mathrm{Im}(E(N) - \mathcal{I}). \tag{4.5}$$

The data reveals the following finite-size scaling behaviour for the normalized eigenvalues:

$$\frac{N}{\pi\xi}(E_r^m - E_0') = R^2(m + \mathrm{i}(x + yN))^2 + r \qquad r \in N \tag{4.6}$$

and the ground state behaves as

$$E_0' = E_0 + \pi\xi \frac{R^2}{N}(x + yN)^2. \tag{4.7}$$

Here m is a quantized number and takes, for odd lattice lengths, the integer values $m = 0, \pm 1, \pm 2, \ldots$, for even lattice lengths half-integer values $m = \pm\frac{1}{2}, \pm\frac{3}{2}, \ldots$. The precise relation between the extrapolants and the constants R, x and y is given by:

$$\begin{aligned} \mathcal{I}_r^m &= 2R^2 my \\ \mathrm{Re}(\mathcal{E}_r^m) &= R^2m^2 + r \\ \mathrm{Im}(\mathcal{E}_r^m) &= 2R^2 mx. \end{aligned} \tag{4.8}$$

Table 3. Extrapolated and predicted values of the energy gaps, computed from the finite-size spectrum of $-H$ for $\alpha = \beta = 0.5$, $q = 0$, $p = 1$ and $r = 0$.

	R^2m^2		$2R^2my$		$2R^2mx$
m	Prediction	Extrapolated	Prediction	Extrapolated	Extrapolated
$\frac{1}{2}$	0.317 648	0.317 63(2)	0.182 104	0.182 104	−0.120 70(3)
1	1.270 594	1.270(6)	0.364 209	0.364 2(1)	−0.241 4(1)
$\frac{3}{2}$	2.858 836	2.858(9)	0.546 313	0.546 313	−0.362 10(7)
2	5.082 375	5.082(3)	0.728 418	0.728(4)	−0.482 8(2)
$\frac{5}{2}$	7.941 211	7.9(4)	0.910 522	0.9(1)	−0.60(4)
3	11.435 343	11.4(8)	1.092 627	1.0(8)	−0.72(3)

Table 4. Data corresponding to (4.8) from the extrapolation of the spectra of $-H$ for $\alpha = \beta = 0.5$, $q = 0$, $p = 1$ with $2 \leqslant N \leqslant 21$; predicted degeneracies are given in square brackets.

	$m = 0$				$m = \frac{1}{2}$		
r	$R^2m^2 + r$	$2R^2mx$	$2R^2my$	r	$R^2m^2 + r$	$2R^2mx$	$2R^2my$
1 [1]	1.000 000			0 [1]	0.317 63(2)	−0.120 70(3)	0.182 104
2 [2]	1.999 99(7)	0.000 0(0)	0.000 00(1)	1 [1]	1.317 65(7)	−0.120 702	0.182 104
3 [3]	3.000 0(0)			2 [2]	2.317(4)	−0.120(7)	0.182 1(1)
	2.999(8)	−0.000(1)	−0.000(0)		2.317 6(8)	−0.120 70(2)	0.182 104
4 [5]	4.000 0(0)			3 [3]	3.3(2)	−0.12(0)	0.182(1)
	4.00(0)	0.000(1)	−0.000(0)		3.317(7)	−0.120 7(0)	0.182 1(0)
	4.0(0)	0.00(3)	−0.00(0)		3.31(7)	−0.120 6(8)	0.182 1(1)
5 [7]	4.99(6)			4 [5]	4.3(2)	−0.1(3)	0.18(4)
	5.00(0)	0.00(0)	0.000(0)		4.31(8)	−0.120(7)	0.182(1)
	5.0(0)	0.0(0)	−0.00(1)		4.317(7)	−0.120(8)	0.182 0(8)
					4.31(6)	−0.12(2)	0.18(2)
6	5.99(7)				4.31(7)	−0.11(8)	0.182(0)
	6.0(1)	0.0(0)	−0.00(1)				
	6.0(0)	0.00(1)	−0.00(0)	5 [7]	5.31(7)	−0.121(4)	0.182 0(8)
	6.0(0)	0.0(0)	−0.00(1)		5.317 4(8)	−0.120(7)	0.182(1)
					5.31(4)	−0.12(2)	0.18(2)
7	7.0(1)				5.31(7)	−0.12(1)	0.18(2)
	6.99(9)	−0.0(0)	−0.000(0)		5.3(2)	−0.1(3)	0.18(4)
	7.0(1)	0.0(0)	−0.00(1)		5.3(2)	−0.11(5)	0.1(8)
8	8.0(0)			6	6.3(1)	−0.11(7)	0.182(1)
	8.0(2)				6.3(4)	−0.1(1)	0.18(1)
	8.0(1)	0.0(0)	−0.00(1)				
	8.(1)	0.(0)	−0.00(5)				
	8.0(1)	0.0(0)	−0.00(1)				
Prediction	0.000 000+r	0.000 000	0.000 000		0.317 648 + r [−0.120 70]		0.182 104

Data for $r = 0$ are shown in table 3. As H is real, we find for each complex eigenvalue E also the complex conjugate E^*. Therefore all tables only show data for $m \geqslant 0$. Data for $r \geqslant 0$ can be found in table 4 for $m = 0$ and $m = \frac{1}{2}$. The corresponding data for $m = 1, \frac{3}{2}, 2, \frac{5}{2}$ and 3 has also been obtained.

The term $\pi\xi I_r^m$, the imaginary part of the energy gaps, takes (independently of α and β) for odd lattice lengths multiples of the same constant 1.8854... that already appeared in the calculation of Gwa and Spohn [6] for the periodic system as the imaginary part of

Table 5. Dependence of the free surface energy f_∞ on α, β.

$\beta \setminus \alpha$	1.5	1.3	1.1	0.9	0.7	0.5	0.3
0.1	0.495 9(9)	0.30(9)	0.123(1)	−0.06(4)	−0.25(6)	−0.463 1(0)	−0.71(0)
0.3	0.908 6(1)	0.722(0)	0.535(8)	0.348(6)	0.156 4(6)	−0.050 216(5)	
0.5	1.156 24(0)	0.969 57(1)	0.783 44(0)	0.596 234(5)	0.404 0372		
0.7	1.362(8)	1.176(2)	0.990 0(9)	0.802 8(9)			
0.9	1.555(0)	1.368(4)	1.18(2)				
1.1	1.742(2)	1.555(6)					
1.3	1.928(3)						

the smallest energy gap. Using Bethe ansatz calculations for the first- and second-smallest eigenvalue in the sector with spin 0 they obtained the following result

$$e_\infty = 0.690\,140\,115 \tag{4.9}$$

$$(E_1 - E_0)_{\text{per}} = 6.577\,678\,7N^{-1} + \mathrm{i}\ 1.885\,456\,427. \tag{4.10}$$

This result can be used to obtain estimates for the parameters R and y, if one assumes that also the spectrum of the periodic chain is characterized by these parameters, and the finite-size scaling of the lowest-lying state with spin 0 is given by [13]

$$\frac{N}{2\pi\xi}(E_1 - E_0)_{\text{per}} = \tfrac{1}{2}R^2 + \mathrm{i}R^2 yN. \tag{4.11}$$

The estimates that have been obtained using this assumption can now be compared with the numerical results. Tables 3 and 4 show a comparison between the values obtained from the analytical calculation and the numerical results. The normalization constant ξ has been taken from numerical Bethe ansatz calculations for the periodical system for up to 80 sites [27]:

$$\xi = 1.647\,843\,926\,946\,23. \tag{4.12}$$

The next constant that has to be determined is the conformal charge c'. The ground-state energy in the thermodynamic limit e_∞ is already known from the periodical system. The surface energy f_∞ can be obtained by extrapolation of

$$f_\infty = \lim_{N\to\infty}(E_0(N) - Ne_\infty). \tag{4.13}$$

The results are given in table 5. Now c can be obtained via

$$c = \lim_{N\to\infty}\frac{24N}{\pi\xi}(E_0(N) - Ne_\infty - f_\infty). \tag{4.14}$$

The numerical values for c are not constant for different values of α and β (see table 6). However, we can shift all energy gaps, independently of the sector by a constant term $24R^2x(\alpha,\beta)^2$ that depends on α and β (table 7). Absorbing this shift into the ground state (see equation (4.7)), one can define a new central charge c'

$$c' = c - 24R^2x^2 \tag{4.15}$$

which is indeed constant within the numerical errors. The numerical values show an excellent agreement with $c' = 1$ (table 6).

Table 6. Extrapolated central charges. The value of R^2x is determined from E_0^1.

$\alpha = \beta$	f_∞	R^2x	c	c'
0.1	−1.12(3)	0.793(8)	12.9(8)	1.0(8)
0.2	−0.6(2)	0.506(0)	5.8(3)	1.0(0)
0.3	−0.297(8)	0.3339(8)	3.1(1)	1.0(1)
0.4	−0.033 6(9)	0.2126(4)	1.84(8)	0.99(4)
0.5	0.197 37	0.1207(0)	1.2752(8)	1.0000(8)
0.6	0.409 65	0.0486(5)	1.044(4)	0.999(7)
0.7	0.610(7)	−0.008(7)	1.00(0)	0.99(9)
0.8	0.804 9(7)	−0.054(6)	1.04(8)	0.99(2)
0.9	1.182 9(2)	−0.0913(7)	1.2(7)	1.1(2)
1.0	1.369(5)	−0.1(2)	1.3(8)	1.1(1)

Table 7. Dependence of R^2x on α and β.

$\beta \setminus \alpha$	1.5	1.3	1.1	0.9	0.7	0.5	0.3
0.1	−0.29(9)	−0.30(9)	−0.32(5)	−0.35(2)	−0.39(3)	−0.459 00	−0.565(6)
0.3	−0.06(8)	−0.07(8)	−0.09(4)	−0.12(1)	−0.1(6)	−0.227 35	
0.5	0.0379(7)	0.028 06	0.011 65	−0.014 67	−0.056 01		
0.7	0.102(5)	0.092(6)	0.076(2)	0.049(9)			
0.9	0.14(3)	0.13(3)	0.11(7)				
1.1	0.17(0)	0.16(0)					
1.3	0.18(6)						

The degeneracies of the energy levels for $r =$ constant are described by the character function of a U(1) Kac–Moody algebra [28]. This confirms the above result $c' = 1$. The Kac–Moody algebra is defined by its commutation relations

$$[T_m, T_n] = m\delta_{m+n,0} \qquad m, n \in Z. \tag{4.16}$$

The character function is given by

$$\chi_{\Delta,q}(z, y) = \mathrm{tr}(z^{L_0} y^{T_0}) = z^{\frac{q^2}{2}} \Pi_V(z) y^q \tag{4.17}$$

where L_0 is a generator of the Virasoro algebra with conformal weight $c = 1$ that can be canonically obtained from the U(1) Kac–Moody algebra using the Sugawara construction [29]. Here q is the eigenvalue of T_0, and the highest weight of L_0 is $\Delta = \frac{q^2}{2}$. A shift in the algebra characterized by a parameter φ

$$\tilde{T}_m = T_m + \varphi\delta_{m,0} \tag{4.18}$$

does not change the commutation relations above but leads to a representation with highest weights

$$\tilde{\Delta} = \tfrac{1}{2}\tilde{q}^2 \qquad \text{where } \tilde{q} = q + \varphi. \tag{4.19}$$

If φ is chosen to be complex, one obtains a representation of the Kac–Moody algebra with negative conformal dimensions. In this case however $\tilde{T}_0^+ \neq \tilde{T}_0$ and the representation is not unitary.

In our case, the energy corrections can be described by a non-unitary representation of a shifted Kac–Moody algebra. The parameter x depends on the boundary terms. The shift φ of the Kac–Moody algebra is given by $\varphi = \sqrt{2}\mathrm{i}R(x + Ny)$.

The results for the antiferromagnetic chain can be summarized in the partition function

$$\mathcal{Z} = z^{-\frac{1}{24}} \sum_{m \in \frac{Z}{2}} z^{R^2(m+\mathrm{i}(x+Ny))^2} \Pi_V(z). \tag{4.20}$$

The operator content of this model corresponds to the one of a Coulomb gas with only magnetic charges and an additional term that depends on the lattice length N. All calculations for $q \neq 0 \neq p$ for $p > q$ show similar results but reveal that in this case x and y are functions of the ratio q/p.

The case $q > p$ has not been studied systematically. Here the observed spectra are purely real, but the convergence of the extrapolations is too bad to obtain precise estimates (the same holds for the case $p = q$, i.e. the symmetric XXZ-chain with additional boundaries).

5. Toy model

In this section we show that a simple model which can be solved analytically has all the features obtained numerically in section 4. We consider the Hamiltonian:

$$H = \sum_{j=1}^{N-1} \sigma_j^+ \sigma_{j+1}^- + \alpha \sigma_1^- + \beta \sigma_N^+. \tag{5.1}$$

For $\alpha = 0$ or $\beta = 0$ the spectrum consists only of the 2^N times degenerate eigenvalue zero. So all the properties of the spectrum come from the boundary terms.

This Hamiltonian can be diagonalized in terms of free fermions. Moreover $H(\alpha, \beta)$ can be transformed into $H(-\alpha, -\beta)$ by applying the transformation $\sigma^\pm \to -\sigma^\pm$. For $\alpha\beta > 0$ the characteristic properties of the spectra described previously are reproduced.

In order to write H in terms of free fermions, we have to obtain a bilinear expression in σ-matrices so that standard fermionization techniques can be applied [30]. Technically, this can be achieved by adding one lattice site at each end of the chain, site 0 and site $N+1$ [31]. The Hamiltonian then reads

$$H' = \sum_{j=1}^{N-1} \sigma_j^+ \sigma_{j+1}^- + \alpha \sigma_0^x \sigma_1^- + \beta \sigma_N^+ \sigma_{N+1}^x. \tag{5.2}$$

As σ_0^x and σ_{N+1}^x commute with H', the spectrum of H' decomposes into four sectors $(++, +-, -+, --)$ corresponding to the eigenvalues ± 1 of σ_0^x and σ_{N+1}^x. We can obtain the eigenvectors of the original problem by projecting onto the $(++)$-sector.

Defining new operators $\tau_j^{+,-} = (\prod_{i<j} \sigma_i^z)\sigma_j^{x,y}$ [32] that obey the anticommutation relations of a Clifford algebra one can rewrite H' as a bilinear expression in τ_j^+ and τ_j^-. Then a linear transformation to new Clifford operators $T_n^\gamma = \sum_{j=0}^{N} \sum_{\mu=\pm 1} (\psi_n^\gamma)_j^\mu \tau_j^\mu$ with $\gamma = \pm 1$ yields

$$H' = \sum_{n=0}^{N+1} \Lambda_n \mathrm{i} T_n^- T_n^+. \tag{5.3}$$

One of the eigenvalues Λ_n is 0, the others are determined by the following equation: $(2\Lambda)^{2N+2} = 4\alpha^2\beta^2(-1)^N$. The solutions are

$$\Lambda_0 = 0 \qquad 2\Lambda_n = (2\alpha\beta)^{\frac{1}{N+1}} (\sin(k) - \mathrm{i}\cos(k)) \tag{5.4}$$

with

$$k = \frac{2n-1}{2N+2}\pi \qquad (0 < n \leqslant N+1). \tag{5.5}$$

Because the operators $\mathrm{i}T_n^- T_n^+$ always have eigenvalues ± 1 it is sufficient to determine the eigenvalues Λ_n with a positive real part. The energy gaps of the spectrum are given by $2\Lambda_n$. For the calculation of the exact ground state, one has to sum all levels with negative energy (so that the fermi sea is full), which leads to

$$E_0 = -\sum_{n=1}^{N+1} \Lambda_n = -\frac{(2\alpha\beta)^{\frac{1}{N+1}}}{2\sin\left(\frac{\pi}{2N+2}\right)}. \tag{5.6}$$

5.1. Scaling of the energy levels

For large N the ground state reads

$$-E_0 \approx \frac{N}{\pi} + \frac{1+\ln(2\alpha\beta)}{\pi} + \frac{\pi}{24N}\left(1 + \frac{12\ln^2(2\alpha\beta)}{\pi^2}\right) + \mathrm{o}(N^{-2}). \tag{5.7}$$

For the study of the low-lying excitations one expands around the minimum of the dispersion relation which is obtained for $k = \pm\frac{\pi}{2}$. For $0 < n \ll N$ one obtains:

$$2\Lambda_{\substack{n \\ N+2-n}} \approx \frac{2n-1}{2}\frac{\pi}{N} \mp \mathrm{i}\left(1 + \frac{\ln(2\alpha\beta)}{N}\right) \qquad \text{for } k \lessgtr \frac{\pi}{2}. \tag{5.8}$$

Up to now we always treated the chain where two additional sites, 0 and $N+1$ have been added to the starting Hamiltonian. We obtain the spectrum of the Hamiltonian without these sites by projection onto the sector where the σ-matrices acting on the additional sites have eigenvalue 1. It can be shown that the spectrum of H with respect to the ground state E_0 is obtained for even N by combining only an odd number of fermions with energies $2\Lambda_n$ and for odd lattice lengths by combining an even number of fermions. The ground state of the system is found to be in the sector with odd lattice lengths.

For the normalization constant, one reads off directly $\xi = 1$.

We turn now to the determination of the partition function because this can be compared directly with previous results. Writing $\tilde{H} = \frac{N}{\pi}(H - E_0)$ and using the triple product identity [33] we obtain

$$\operatorname{tr} z^{\tilde{H}} = \prod_{n=1}^{\infty}(1 + z^{n-\frac{1}{2}}z^{\mathrm{i}a})(1 + z^{n-\frac{1}{2}}z^{-\mathrm{i}a}) = \sum_{m\in\frac{Z}{2}} z^{2(m+\mathrm{i}\frac{a}{2})^2+\frac{a^2}{2}} \prod_{n=1}^{\infty}(1-z^n)^{-1} \tag{5.9}$$

with

$$\frac{a}{2} = x + yN \qquad x = \frac{\ln(2\alpha\beta)}{2\pi} \qquad y = \frac{1}{2\pi}. \tag{5.10}$$

Here we obtain $m \in Z$ for odd lattice lengths and $m \in Z + \frac{1}{2}$ for even lattice lengths. Absorbing the term $\frac{a^2}{2}$ into the ground-state energy, we get the following expression:

$$E_0'(N) = -\frac{N}{2\pi} - \frac{1}{\pi} - \frac{\pi}{24N} + \mathrm{o}(N^{-2}). \tag{5.11}$$

This corresponds to a system with conformal charge $c = 1$. For the partition function we obtain

$$\mathcal{Z} = z^{-\frac{1}{24}} \sum_{m \in \frac{Z}{2}}^{\infty} z^{2(m+\mathrm{i}(x+Ny))^2} \prod_{n=1}^{\infty} (1 - z^n)^{-1}. \tag{5.12}$$

This is exactly the same result obtained numerically in section 4 for $R^2 = 2$.

Comparing the partition function for the toy model with those for the open and for the periodic XXZ-chain [13, 34, 35] we get some insight into the nature of the different new terms in the partition function. For asymmetric XXZ-chains with diagonal boundary conditions one gets the spectrum of a Coulomb gas with electric charges. In the case of non-diagonal boundary terms we get only magnetic charges. These boundary conditions also give rise to an imaginary shift $\mathrm{i}x$ in the magnetic charges that also appear for the periodic chain with a real twist [34]. In our case x depends on the product $\alpha\beta$.

6. Conclusions

In this paper, we have studied the spectrum of the asymmetric XXZ-chain with non-Hermitian boundary terms. Numerical methods have been applied for the determination of the eigenvalues. Analytically, we studied a toy model that reproduces the characteristic properties of the full antiferromagnetic Hamiltonian. In two different cases, we concluded that the boundary terms induce the phase transitions of the Hamiltonian.

We studied first the ferromagnetic chain with $\alpha, \beta > 0$ that describes the time evolution of a reaction-diffusion system with asymmetric diffusion in the bulk and additional injection and extraction terms at the boundaries. For the completely asymmetric chain the behaviour of the smallest energy gap that corresponds directly to the inverse temporal correlation length shows the same behaviour as the spatial correlation length in the stationary state determined by [2, 3]. In phases A and B where the spatial correlation length stays finite, i.e. the concentration of particles shows an exponential decay in the spatial direction, we find a massive spectrum where the mass depends on the same parameters as the spatial correlation length in the different phases A_1, A_2, B_1 and B_2. In this way the subdivision of phases A and B is also valid for the dynamical properties of H. However, the numerical values of the spatial and the temporal correlation lengths do not coincide. Phase C, where the spatial density profile of the stationary state decays algebraically in the thermodynamic limit, exhibits a divergence of the temporal correlation length with an exponent $\frac{3}{2}$ for $N \to \infty$. This exponent has already been identified for the model with periodic boundary conditions. On the coexistence line, we find a divergence with an exponent 2. These results did not come as a surprise.

The antiferromagnetic chain for $\Delta < -1$ shows unexpected features. For $\alpha = 0$ or $\beta = 0$ the spectrum corresponds to that of a XXZ-chain with additional σ^z-terms at the boundaries and therefore is massive. Only when both α and β are non-zero, is the spectrum massless and can be described by the partition function

$$\mathcal{Z} = z^{-\frac{1}{24}} \sum_{m \in \frac{Z}{2}} z^{R^2(m+\mathrm{i}(x+Ny))^2} \Pi_V(z) \tag{6.1}$$

with magnetic charges only. The analysis of the toy model that was diagonalized in terms of free fermions reproduces the same structure of the spectrum. The length-dependent term seems to be a common property of the anisotropy of the spin chain [26] and also appeared for the periodic chain [13]. The imaginary shift of the magnetic charge is an effect of

the non-Hermitian and non-diagonal boundary terms. The influence of more general non-diagonal boundary terms and asymmetric interactions in the bulk will be the subject of a future publication [36].

Acknowledgments

We wish to thank Professor V Rittenberg for suggesting this interesting problem and for enlightening discussions and constant support. We are very grateful to Professor D Kim and G Schütz for valuable discussions and suggestions. We wish to thank the whole group for constant help and discussions.

References

[1] Sandow S 1994 *Phys. Rev.* **E50** 2660
[2] Derrida B, Evans M R, Hakim V and Pasquier V 1993 *J. Phys. A: Math. Gen.* **26** 1493
[3] Schütz G and Domany E 1993 *J. Stat. Phys.* **72** 277
[4] Derrida B, Domany E and Mukamel D 1992 *J. Stat. Phys* **69** 667
[5] Essler H L and Rittenberg V 1996 *J. Phys. A: Math. Gen.* **29** 3375
[6] Gwa L and Spohn H 1992 *Phys. Rev.* A **46** 844
[7] Kim D 1995 *Phys. Rev.* E **52** 3512
[8] de Vega H J and Gonzales-Ruiz A 1994 *J. Phys. A: Math. Gen.* **27** 6129
Inami T and Konno H 1994 *J. Phys. A: Math. Gen.* **27** L913
[9] Alcaraz F C, Droz M, Henkel M and Rittenberg V 1994 *Ann. Phys., NY* **230** 250
[10] Sutherland B 1967 *Phys. Rev. Lett.* **19** 103
Lieb E and Wu F Y 1972 in *Phase Transitions and Critical Phenomena* vol 1 (London: Academic)
[11] van Beijeren H 1977 *Phys. Rev. Lett.* **38** 993
Jayaprakash C and Saam W F 1984 *Phys. Rev.* B **30** 3916
Jayaprakash C, Saam W F and Teitel S 1983 *Phys. Rev. Lett.* **50** 2017
Bukman D J and Shore J D 1995 *J. Stat. Phys.* **78** 1277
[12] Albertini G, Dahmen S R and Wehefritz B 1996 *J. Phys. A: Math. Gen.* **29** L369
[13] Noh J D and Kim D 1995 *Phys. Rev.* E **53** 3225
[14] Saad Y 1980 *Linear Algebra Appl.* **34** 269
Saad Y 1981 *Math. Comput.* **37** 105
Saad Y 1992 *Numerical Methods for Large Eigenvalue Problems* (Manchester: Manchester University Press)
[15] Yildirim K 1995 *Diplomarbeit* BONN-IB-95-02
[16] von Gehlen G 1994 *Int. J. Mod. Phys.* **8** 3507
[17] Di Francesco P, Saleur H and Zuber I-B 1987 *Nucl. Phys.* B **285** 454
Nienhuis B 1987 *Phase Transitions and Critical Phenomena* vol 11 (London: Academic Press)
[18] Kadanoff L P and Swift J 1968 *Phys. Rev.* **165** 310
[19] Pasquier V and Saleur H 1990 *Nucl. Phys.* B **330** 523
[20] Burlisch R and Stoer J 1964 *Numer. Math.* **6** 413
Henkel M and Schütz G 1988 *J. Phys. A: Math. Gen.* **21** 2617
[21] See, for example, Krug J and Spohn H 1991 *Solids Far From Equilibrium: Growth, Morphology and Defects* ed C Godrèche (Cambridge: Cambridge University Press) and references therein
[22] Kardar M, Parisi G and Zhang Y C 1986 *Phys. Rev. Lett.* **56** 889
[23] Andjel E D, Bramson M D and Liggett T M 1988 *Probab. Theor. Rel. Fields* **78** 231
Ferrari P A and Fontes L R G 1994 *Probab. Theor. Rel. Fields* **99** 305
Derrida B, Evans M R and Mallick K 1995 *J. Stat. Phys.* **79** 833
[24] Schütz G 1993 *Phys. Rev.* E **47** 4265
[25] Cardy J L 1988 *Fields, Strings and Critical Phenomena (Les Houches 1988)* (Amsterdam: North-Holland)
[26] Kim D and Pearce P 1987 *J. Phys. A: Math. Gen.* **20** L451
[27] Dahmen S R and Wehefritz B unpublished
[28] Goddard P and Olive D 1986 *Int. J. Mod. Phys.* A **1** 303
[29] Corrigan E 1986 *Phys. Lett.* **169B** 259
[30] Lieb E, Schultz T and Mattis D 1961 *Ann. Phys.* **16** 407
[31] Hinrichsen H, Krebs K and Peschel I 1996 *Z. Phys.* B **100** 105

[32] Hinrichsen H 1994 *J. Phys. A: Math. Gen.* **27** 5393
[33] Ginsparg P 1988 *Fields, Strings and Critical phenomena (Les Houches 1988)* (North-Holland: Amsterdam)
[34] Alcaraz F C, Baake M, Grimm U and Rittenberg V 1988 *J. Phys. A: Math. Gen.* **21** L117
[35] Alcaraz F C, Barber M N and Batchelor M T 1987 *Phys. Rev. Lett.* **58** 771
Hamer C J, Quispel G R W and Batchelor M T 1987 *J. Phys. A: Math. Gen.* **20** 5677
Alcaraz F C, Barber M N, Batchelor M T, Baxter R J and Quispel G R W 1987 *J. Phys. A: Math. Gen.* **20** 6397
Hamer C J and Batchelor M T 1988 *J. Phys. A: Math. Gen.* **21** L173
Alcaraz F C, Barber M N and Batchelor M T 1988 *Ann. Phys* **182** 280
Alcaraz F C and Wreszinski W F 1990 *J. Stat. Phys* **58** 45
[36] Bilstein U and Wehefritz B in preparation